Proceedings of the XVII ECSMGE-2019
Geotechnical Engineering foundation of the future
ISBN 978-9935-9436-1-3

doi: 10.32075/17ECSMGE-2019-0671

XVII European Conference
ECSMGE 2019
Reykjavik
on Soil Mechanics
and Geotechnical Engineering

Modelling the geomembrane – fly ash interface behaviour

Modélisation du comportement de l'interface géomembrane – cendres volantes

R. Aza-Gnandji
University of Cape Town, South Africa

D. Kalumba
University of Cape Town, South Africa

V. Gbaguidi
University of Abomey-Calavi, Benin

ABSTRACT: In South Africa, it is estimated that more than 25 million tons of fly ash are produced annually by the coal-fired power stations deployed to satisfy the high demand of electricity. These huge deposits of fly ash constitute an environmental problem whenever their chemical constituents leak and contaminate underlying aquifers in areas where they are disposed. To avoid such contamination and to protect the aquifers, barriers comprising geosynthetic materials such as geomembranes and geosynthetic clay liners are often placed underneath or between the fly ash deposits. In this paper, a numerical model was developed to simulate the shear strength versus shear displacement responses of the geomembrane – fly ash interfaces. A series of large direct shear tests were first conducted to study experimentally the behaviour of the interface between geomembrane and fly ash produced locally. Then, the experimental data were used for the numerical model developed in Matlab R2017a to simulate the behaviour of the geomembrane – fly ash interface. The considered numerical schemes showed good agreement between the experimental and the numerical data. Based on the results obtained, the technique implemented is recommended for the analysis of the shear strength versus shear displacement responses of the geomembrane – fly ash interfaces.

RÉSUMÉ: En Afrique du Sud, it est estimé que les centrales thermiques au charbon déployées pour satisfaire la forte demande en énergie électricique produisent annuellement plus de 25 millions de tonnes de cendres volantes. Ces énormes dépôts de cendres volantes constituent un problème environnemental chaque fois que leurs constituants chimiques s'infiltrent et contaminent les aquifères sous-jacents dans les zones où ils sont entassés. Pour éviter cette contamination et protéger les aquifères, des barrières constituées de matériaux géosynthétiques tels que les géomembranes et les couches d'argile géosynthétiques sont souvent placées sous ou entre les dépôts de cendres volantes. Dans cet article, un modèle numérique a été développé pour simuler les résultats de la resistance au cisaillement en fonction du déplacement sous cisaillement direct des interfaces géomembrane – cendres volantes. Une série d'essais de cisaillement direct à la grande boîte a d'abord été réalisée pour étudier expérimentalement le comportement de l'interface entre la géomembrane et les cendres volantes produites localement. Ensuite, les données expérimentales ont été utilisées pour le modèle numérique développé dans Matlab R2017a pour simuler le comportement de l'interface géomembrane – cendres volantes. Les approches numériques considérés ont montré une bonne corrélation entre les données expérimentales et numériques. Sur la base des résultats obtenus, la technique mise en œuvre est recommandée pour l'analyse de la résistance au cisaillement en fonction du déplacement en cisaillement des interfaces géomembrane – cendres volantes.

Keywords: Fly Ash; Geomembrane; Interface; Shear Strength; South Africa

1 INTRODUCTION

Worldwide, the consumption of electricity has increased during the last decades. This high demand is primarily due to the population increase and the intense urbanization that is occurring in many countries. Although new sources for the generation of electricity are being explored and developed, the ongoing sources such the coal-fired power stations are still greatly used to meet the high need in electricity. The operation of these power stations produces unfortunately huge deposits of fly ash which constitute an environmental problem whenever their chemical constituents leak and contaminate underlying aquifers in areas where they are dumped (Fatoba, 2010). In South Africa, it is estimated that more than 25 million tons of fly ash are produced annually by the coal-fired power stations due to the high demand of electricity (Eskom, 2017). To avoid such contamination and to protect the natural resources, geotechnical engineers and environmental scientists usually revert to barriers comprising geosynthetic materials such as geomembranes and geosynthetic clay liners that are placed underneath or between the fly ash deposits. Despite these measures, contamination still happens since ruptures of these geosynthetic materials sometimes occur upon loading in some conditions. Examples of these failures include the failure of the hazardous waste landfill in 1988 at Kettleman Hills in USA (Mitchell et al., 1990); and the geomembrane rupture which occurred during the Northridge earthquake in 1994 at the Chiquita Canyon landfill in USA (Kavazanjian et al., 2012).

To prevent the rupture of these geosynthetic materials and to maintain their integrity, a variety of studies are conducted to enable the design of more resistant geosynthetic materials, and for the better understanding of the mechanical behaviour of the soil-geosynthetic and geosynthetic-geosynthetic interfaces under different loading conditions. Among others, such studies include research on the experimental and numerical estimations of the shear strength properties of the soil-geosynthetic or geosynthetic-geosynthetic interfaces subjected to either monotonic or cyclic loading, and case studies on landfills designed with geosynthetic lining systems through slope stability analyses (Bergado et al., 2006; Bacas et al., 2011; Vieira et al., 2013).

Numerical simulations of the design of geosynthetic lining systems offer the possibility to study the influence of different parameters on their performance, and reliable numerical analyses require proper modelling of the geosynthetic – soil interfaces. Esterhuizen et al. (2001) developed a numerical method for the analysis of the geomembrane – clay interfaces and they recommended the use of their numerical technique for the analysis of soil-geosynthetic interfaces showing similar behaviour. Through a recent work, Anubhav and Basudhar (2010) found that their proposed numerical technique was not totally suitable for the analysis of the behaviour of geotextile – sandy soil interfaces, and they then proposed a modified approach. In this study, the numerical technique proposed by Anubhav and Basudhar (2010) was used to simulate the shear strength versus shear displacement responses of geomembrane – fly ash interfaces. A series of large direct shear tests of the interfaces between compacted fly ash and three different geomembranes were first conducted in a geotechnical laboratory, and the experimental results were then compared with the numerical ones obtained through the procedures presented in this paper.

2 EXPERIMENTAL STUDY

2.1 Test materials

The fly ash used for the present study was sourced from one of the coal-fired power stations in South Africa. Its particle size distribution revealed that it was predominantly silt size since it consisted of 17% of particles with size greater than 0.075 mm, 73% of particles with size

between 0.002 mm and 0.075 mm, and 10% of particles less than 0.002 mm. The specific gravity of the fly ash was 2.34. The maximum dry density of the fly ash was 1.13 Mg/m^3 and the corresponding optimum water content was 40.7%.

Three types of geomembrane were used during the shear tests of the interfaces between the tested fly ash and the geomembranes for this work. They were all High-Density Polyethylene (HDPE) geomembranes with 1.5 mm core thickness. GeombA was a non-textured geomembrane, while GeombB and GeombC were textured geomembranes with specific patterns. Table 1 gives a summary of their engineering properties.

2.2 Test procedure

The Automated Shear Trac III Large-scale Direct Shear device produced by GEOCOMP following the standard (ASTM, 2008) was the direct shear apparatus used in this study (Figure 1). The shear box consisted of an upper box, 305 mm x 305 mm in the horizontal plan and 100 mm in height, and a lower box, 305 mm x 405 mm in the horizontal plan and 100 mm in height. The upper box was fixed in the horizontal direction, while the lower box moved horizontally and was driven by the electric motors.

To perform the tests, the geomembrane specimens with horizontal dimensions of 310 mm x 410 mm were cut from the roll, and placed on the lower box which was filled with mild steel of 100 mm high. The fly ash mixed with water quantity corresponding to the optimum water content, was placed in layers and compacted to a density close to its maximum dry density as determined by the compaction test. The test samples were sheared at normal stresses equal to 20, 200 and 400 kPa, with a shear displacement rate of 1 mm/min. These normal stresses were selected so as to represent the different overburden pressures that could be applied to the interfaces. At the end of each test, the equipment automatically generated the variation of the shear stress against the shear displacement for each applied normal stress which was then used during data processing and analysis.

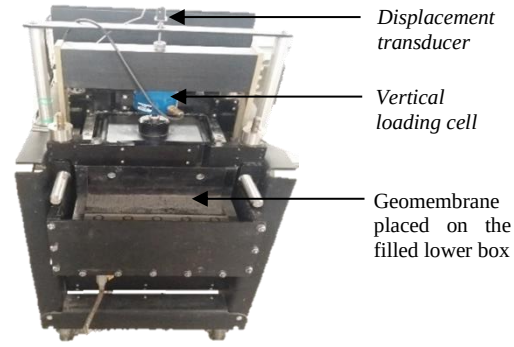

Figure 1. Automated Shear Trac III Large-scale Direct Shear equipment used during the interface tests

2.3 Test results

The curves of the shear stress versus the shear displacement are shown in Figure 2 for the three geomembrane – fly ash interfaces. For all the interfaces, the shear displacement necessary to mobilize the peak shear strength increased with higher applied normal stress. The GeombB – Fly ash interface showed a fast reduction in shear strength after the peak shear stress was reached for the third applied normal stress (400 kPa). This behaviour was again obtained when this test was repeated. This observed behaviour could be due to the surface texture of the geomembrane B. It is also observed that more shear strength was mobilized to reach failure for the GeombC – Fly ash as compared to the other interfaces. This suggests that the geomembrane C could resist to higher load than the others.

The variation of the peak shear stresses with the normal stresses for the three types of geomembrane are shown in Figure 3. For the GeombA – Fly ash interface, the secant friction angles were 38°, 36° and 28° for the applied normal stress 20, 200 and 400 kPa respectively. Similarly, they were 45°, 38° and 36° for the GeombB – Fly ash interface, and 61°, 38° and 40° for the GeombC – Fly ash interface respectively. These values of secant friction angle decreased generally with the increasing normal stresses.

Table 1. Engineering properties of the geomembranes used (obtained from the suppliers' technical brochures)

Geomem-brane	Thick-ness (mm)	Asperity Height (mm)	Density (g/cm^3)	Tensile strength at (N/mm)		Elongation at (%)		Tear resistance (N)	Puncher resistance (N)
				Yield	Break	Yield	Break		
GeombA (HDS150)	1.50	---	0.940	22	45	13	700	187	520
GeombB (HDT150)	1.50	0.25	0.940	22	25	12	400	187	440
GeombC (HST150)	1.50	0.25	0.940	22	25	12	400	187	440

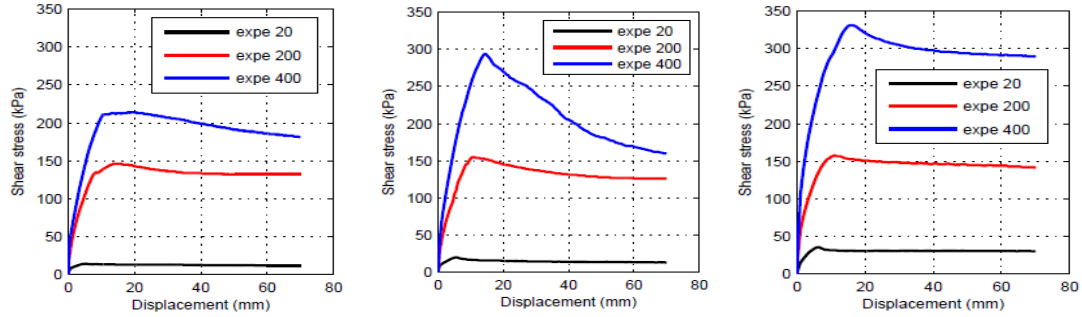

(a) GeombA – Fly ash interface (b) GeombB – Fly ash interface (c) GeombC – Fly ash interface

Figure 2. Shear stress vs horizontal displacement for the geomembrane – fly ash interfaces

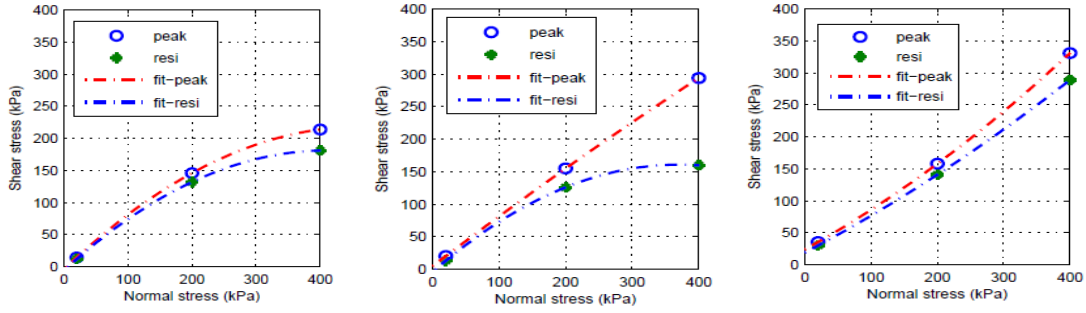

(a) GeombA – Fly ash interface (b) GeombB – Fly ash interface (c) GeombC – Fly ash interface

Figure 3. Shear strength vs normal stress for the geomembrane – fly ash interface

Table 2. Values of coefficients a, b, c

Interface	Peak shear stresses			Residual shear stresses		
	a	*b*	*c*	*a*	*b*	*c*
GeombA – fly ash	0.0005	0.5729	23.8474	0.0003	0.5435	19.1988
GeombB – fly ash	-0.0001	0.7792	4.7719	-0.0012	0.8911	-4.1404
GeombC – fly ash	-0.0010	0.9575	-4.3392	-0.0011	0.9108	-5.7719

3 NUMERICAL STUDY

The numerical technique developed by Anubhav and Basudhar (2010) to simulate the behaviour of geosynthetic – sand interfaces was used to simulate the entire shear stress – displacement response of the interfaces between the tested geomembranes and fly ash in this work. The complete behaviour was divided in two parts namely pre-peak behaviour and post-peak behaviour. Non-linear failure envelopes were used to obtain the peak and the residual shear stresses.

3.1 Pre-peak behaviour

The variation of the shear stress with the shear displacement in Figure 2 shows that the initial shear stiffness depends on the applied normal stress, and that the tangent shear modulus changes with the displacement. To model the pre-peak behaviour, the technique proposed by Duncan and Chan (1970), and Duncan et al. (1980), which was modified by Anubhav and Basudhar (2010) was followed. The non-linear behaviour of the geomembrane – fly ash interface was represented by a hyperbolic equation in the form proposed by Kondner (1963):

$$\tau = \frac{d}{\frac{1}{E_i} + \frac{d}{\tau_{ult}}} \quad (1)$$

Where:

τ : Shear stress.

d : Shear displacement.

E_i : Initial tangent shear modulus.

τ_{ult} : Ultimate shear stress.

The equation suggested by Junbu (1963) was used to express the variation of E_i with σ_n .

$$E_i = KP_a\left(\frac{\sigma_n}{P_a}\right)^n \quad (2)$$

Where:

σ_n : Applied normal stress.

K: Modulus number (dimensionless number).

n: Modulus exponent (dimensionless number).

P_a : Atmospheric pressure.

The variation of the ultimate shear stress (τ_{ult}) with the normal stress was considered by relating it with the peak shear stress (τ_p) as follows:

$$\tau_p = R_f\tau_{ult} \quad (3)$$

Where:

R_f is the failure ratio which is always less than 1 since τ_p is always smaller than τ_{ult} (Duncan et al., 1980; Konder, 1963).

To obtain the values of the coefficients K, n and R_f, the procedure explained in the research of Duncan et al. (1980) was followed for their determination.

Contrary to the linear failure envelope represented by the Mohr-Coulomb criterion used in the technique proposed by Anubhav and Basudhar (2010) to estimate the peak and residual shear stresses for the geosynthetic interfaces, a non-linear failure envelope was considered in this research for their estimation. This approach was in line with the studies conducted by Esterhuizen et al. (2001), Eid (2011) and Kavazanjian et al. (2012) who observed that the experimental tests on the behaviour of geosynthetic – soil interface usually exhibit non-linear shear stress versus normal stress relationship. For this study, the considered non-linear expression was as follows:

$$\tau = a\sigma_n^2 + b\sigma_n + c \quad (4)$$

Where:

$a, b, and\ c$: are coefficients obtained through a curve fitting technique with the experimental data shown in Figure 3. Table 2 provides a summary of these coefficients found with good fits (R^2 values were equal to 0.99 for all geomembrane – fly interfaces).

σ_n : Applied normal stress.

τ : Peak or Residual shear stress.

3.2 Post-peak behaviour

For this study, the modified approach proposed by Anubhav and Basudhar (2010) which accounts for the slow decrease of the shear strength in the initial stages after the peak, was considered for the simulation of the post-peak behaviour. The technique was preferred as the experimental data exhibited shear strength vs shear displacement curves similar to the general curve depicted in Figure 4. The post-peak shear strength reduction $(\tau_p - \tau)$, and the post-peak plastic shear displacement (dp) are shown in Figure 4. The post-peak shear strength is limited by the peak shear strength and the residual shear strength. The post-peak shear strength reduction $(\tau_p - \tau)$ is normalized by the shear strength reduction from peak to the residual value

$(\tau_p - \tau_r)$ defined by the residual factor (ReF) proposed by Skempton (1954) which was:

$$ReF = \frac{\tau_p - \tau}{\tau_p - \tau_r} \quad (5)$$

Where:

τ_p : Peak shear stress.

τ_r : Residual shear stress.

τ : Shear stress obtained after the peak shear stress is reached.

The plots of the residual factor versus the plastic shear displacement were then correlated with fitted curves which can be represented by the equation proposed by Anubhav and Basudhar (2010) as follows:

$$ReF = 1 - \exp(-Ad_p^z) \quad (6)$$

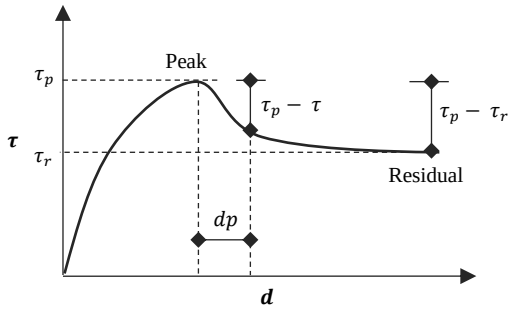

Figure 4. Generalized stress-displacement relationship for geosynthetic interfaces (Anubhav and Basudhar, 2010)

3.3 Model parameters

Following the procedure described in the previous sections, the variation of the pre-peak behaviour of the shear strength with shear displacement of the fly ash – geomembrane interfaces was obtained. Three parameters namely $K, R_f,$ and n were necessary to represent the pre-peak behaviour; and two parameters namely A and z were required for the simulation of the post-peak behaviour. The two latter parameters were obtained through a non-linear regression analysis using Matlab R2017a while first plotting the computed residual factors with the experimental data in function of the plastic shear displacement defined previously, and then correlating these residual factors with the fitted curves represented by equation 6. Figure 5 shows good fits that were obtained between the experimental values and the fitted curves (R^2 values were equal to 0.8, 0.9 and 0.7 for GeombA – Fly ash, GeombB – Fly ash and GeombC – Fly ash interfaces respectively). Table 3 summarizes the model parameter values obtained through the outlined procedure required for the complete simulation of the behaviour of shear strength vs shear displacement of the geomembrane – fly ash interfaces.

4 COMPARISON BETWEEN THE EXPERIMENTAL AND NUMERICAL RESULTS

Figure 6 depicts the variation of the shear strength with the shear displacement for both the experimental data and the numerical data obtained through a back-fitting analysis performed in Matlab R2017a. As it can be seen, the numerical data exhibited good agreement with the experimental data. The modified approach proposed by Anubhav and Basudhar (2010) used in this study provided a good simulation of the entire behaviour of the geomembrane -fly ash interfaces. The approach enabled to represent both the slow and the fast decrease in the initial stages after the peak shear strength was attained. This numerical approach originally developed for the analysis for sand-geotextile interfaces has shown to a good extend its effectiveness in the simulation of the shear stress versus shear displacement responses of the interface between the tested fly ash and geomembranes considered in this work.

5 CONCLUSIONS

In this study, a numerical model was developed for the simulation of shear stress versus shear displacement response of the interface between fly ash and three different geomembranes. Large

Table 3. Model parameters for the complete behaviour

Interface	Pre-peak parameters		Post-peak parameters		
	K	R_f	n	A	z
GeombA – fly ash	423.743	0.837	0.383	0.029	1.130
GeombB – fly ash	322.664	0.717	0.418	0.048	1.044
GeombC – fly ash	528.728	0.809	0.516	0.210	0.632

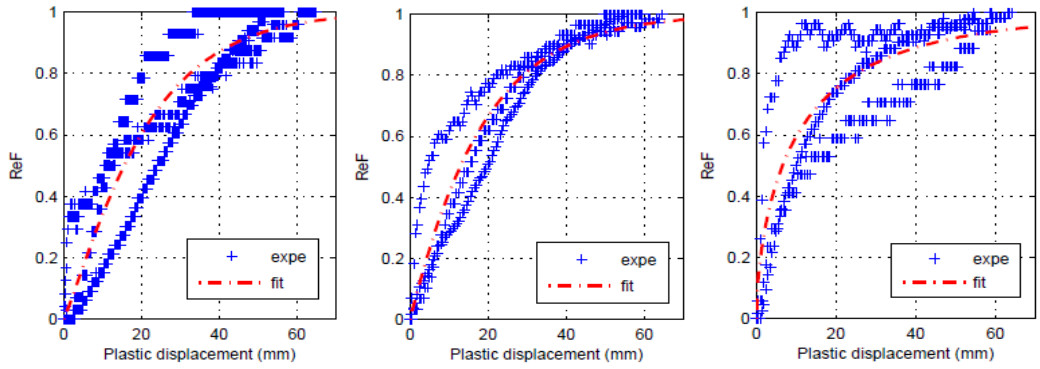

(a) GeombA – fly ash interface (b) GeombB – fly ash interface (c) GeombC – fly ash interface

Figure 5. Variation of the residual factor with the plastic displacement

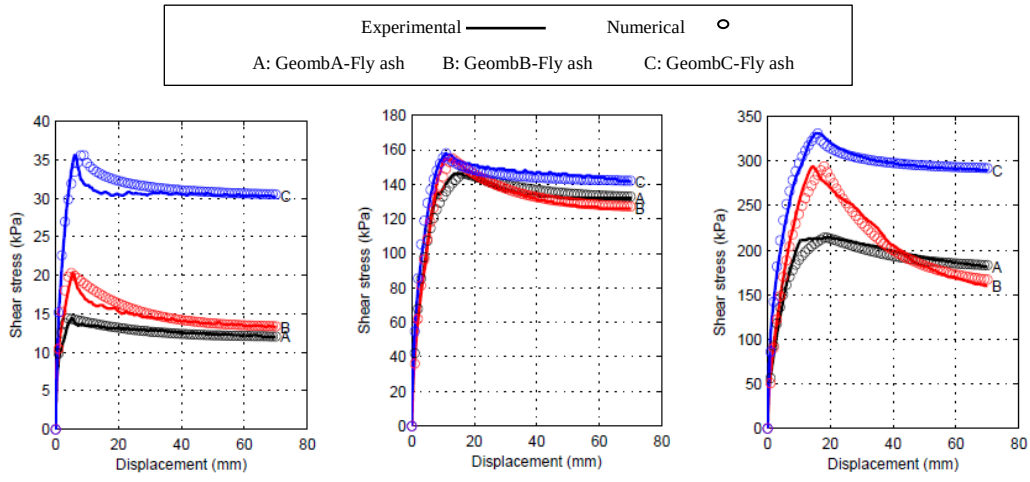

(a) Normal stress (20 kPa) (b) Normal stress (200 kPa) (c) Normal stress (400 kPa)

Figure 6. Variation of the shear strength vs shear displacement for the geomembrane – fly ash interfaces

direct shear tests were first performed in a geotechnical laboratory, and the experimental data were then used for the calibration of the numerical technique. The shear displacement necessary to mobilize the peak shear strength increased with higher applied normal stress. The values of the secant friction angle decreased with the increasing normal stresses for the interfaces between the fly ash and the geomembranes tested. In terms of load bearing and resistance, GeombC – Fly ash interface exhibited more resistance to failure and had higher values of the secant friction angle.

In the numerical technique, the shear strengths along the geomembrane interfaces were better estimated using a non-linear relationship. Although originally developed for the analysis of the behaviour of sand – geotextile interfaces, the followed numerical approach showed a good agreement between the experimental and the numerical data for the analysis of the behaviour of geomembrane – fly ash interfaces since good fits with the experimental data were obtained. Based on the findings of this work, it can be recommended the use of this numerical approach for the analysis of behaviour of interface along geosynthetic materials which may exhibit similar behaviour.

6 ACKNOWLEDGEMENTS

The authors would like to thank the University of Abomey-Calavi, and the Geotechnical Engineering Research Group at the University of Cape Town for their valuable financial support.

7 REFERENCES

Anubhav and Basudhar P.K. 2010. *Modeling of soil–woven geotextile interface behavior from direct sheartest results*. Geotextiles and Geomembranes 28 403–408.

ASTM D 5321. 2008. *Standard Test Method for Determining the Coefficient of Soil and Geosynthetic or Geosynthetic and Geosynthetic Friction by Direct Shear Method*. American Society for Testing and Materials.

Bacas B. M., Konietzky H., Berini J. C., Sagaseta C. 2011. *A new constitutive model for textured geomembrane/geotextile interfaces*. Geotextiles and Geomembranes 29 137 – 148 .

Bergado D.T., Ramana G.V., Siaa H.I., Varun. 2006. *Evaluation of interface shear strength of composite liner system and stability analysis for a landfill lining system in Thailand*. Geotextiles and Geomembranes 24, 371–393.

Duncan, J.M., Chan, C.Y. 1970. *Nonlinear analysis of stress and strain in soils*. Journal of Soil Mechanics and Foundations Division, ASCE 96 (SM 5), 1629–1653 .

Duncan J. M., Byrne P., Wong K. S. and Mabry P. 1980. *Strength, stress-strain and bulk modulus parameters for finite element analysis of stresses and movements in soil masses*. Report N0 UCB/GT/80-01, University of California-Berkeley, USA.

Eid H. T. 2011. *Shear strength of geosynthetic composite systems for design of landfill liner and cover slopes*. Geotextiles and Geomembranes 29 335 – 344.

Eskom Homepage, http://www.eskom.co.za/news/Pages/Feb20.aspx, Eskom and Ash management, last accessed 2017/04/18.

Esterhuizen, J.J.B., Fliz, G.M., Duncan, J.M. 2001. *Constitutive behavior of geosynthetic interface*. Journal of Geotechnical and Geoenvironmental Engineering, ASCE 127 (10), 834–840.

Fatoba O. O. 2010. *Chemical interactions and mobility of species in fly ash – brine co-disposal systems*. Ph.D. thesis, University of the Western Cape, South Africa.

Janbu, N. 1963. *Soil compressibility as determined by oedometer and triaxial tests*. In: Proc. European Conf. on Soil Mechanics and Foundation Engineering, Wiesbaden, Germany, vol. 1, pp. 19–25 .

Kavazanjian E., Arab M. and Matasovic N. 2012. *Performance based design for seismic design of geosynthetics-lined waste containment systems*. In: Second International Conference on Performance-Based Design in Earthquake Geotechnical Engineering, Toormina, Italy.

Kondner, R.L. 1963: *Hyperbolic stress–strain response: cohesive soils*. Journal of Soil Mechanics and Foundations Division, ASCE 89 (1) 289–324.

Mitchell, J.K., Seed, R.B., Seed, H.B. 1990: *Kettleman Hills waste landfill slope failure. I: Liner-system properties*. ASCE Journal of Geotechnical Engineering 116 (4) 647–668.

Vieira C. S., Lopes M. L. and Caldeira L. M. 2013. *Sand-geotextile interface characterisation through monotonic and cyclic direct shear tests*. ICE Publishing, Geosynthetics International 20 No. 1.

Skempton, A.W. 1964: *Long term stability of clay slopes*. Geotechnique 14 (2), 77–101.